

# RSC Advances



This is an *Accepted Manuscript*, which has been through the Royal Society of Chemistry peer review process and has been accepted for publication.

*Accepted Manuscripts* are published online shortly after acceptance, before technical editing, formatting and proof reading. Using this free service, authors can make their results available to the community, in citable form, before we publish the edited article. This *Accepted Manuscript* will be replaced by the edited, formatted and paginated article as soon as this is available.

You can find more information about *Accepted Manuscripts* in the [Information for Authors](#).

Please note that technical editing may introduce minor changes to the text and/or graphics, which may alter content. The journal's standard [Terms & Conditions](#) and the [Ethical guidelines](#) still apply. In no event shall the Royal Society of Chemistry be held responsible for any errors or omissions in this *Accepted Manuscript* or any consequences arising from the use of any information it contains.

## Quantitative proteomic analysis of synovial tissue from rats with collagen-induced arthritis

Wei Huang<sup>ab</sup>, Qinghua Liang<sup>ab</sup>, Jiang Chen<sup>c</sup>, Hao Zhu<sup>d</sup>, Wei Xie<sup>e</sup>, Yang Wang<sup>ab</sup>, Bo Yang<sup>ab</sup>, Weijun Peng<sup>a</sup>, Xingui Xiong<sup>ab\*</sup>

<sup>a</sup> Institute of Integrated Medicine, Xiangya Hospital, Central South University, No. 87 Xiangya Road, Changsha, Hunan 410008, P R China.

<sup>b</sup> Key Laboratory of Chinese Gan of State Administration of Traditional Chinese Medicine, Changsha, 410008, China.

<sup>c</sup> Central of Telemedicine, Xiangya Hospital, Central South University, No. 87 Xiangya Road, Changsha, Hunan 410008, P R China.

<sup>d</sup> Institute of Integrated Medicine, the first affiliated hospital of Soochow university, No.188 Shizi Street, Soochow, Jiangsu, 215006, P R China.

<sup>e</sup> Department of Pathology & Immunology, Baylor College of Medicine, One Baylor Plaza, BCM 315, Houston, 77030, US.

Email address:

Huang Wei(huangweidavid@aliyun.com )

Qinghua Liang(lqhxy@126.com)

Jiang Chen(cjxyz@126.com)

Hao Zhu(tom.grade@126.com)

Wei Xie (Wei.Xie2@bcm.edu)

Yang Wang(xiaoyangge02@126.com)

Bo Yang (yangbo05@gmail.com)

Weijun Peng (Pengweijun87@gmail.com)

Xingui Xiong(xiongxg07@gmail.com)

Addresses Correspondence to:

Institute of Integrated Medicine, Xiangya Hospital, Central South University, No. 87 Xiangya Road, Changsha, Hunan 410008, P R China. Tel: +86-731-84327569 Fax:086-731-84327568; Email: xiongxg07@gmail.com

## Quantitative proteomic analysis of synovial tissue from rats with collagen-induced arthritis †<sup>1</sup>

Wei Huang<sup>ab</sup>, Qinghua Liang<sup>ab</sup>, Jiang Chen<sup>c</sup>, Hao Zhu<sup>d</sup>, Wei Xie<sup>e</sup>, Yang Wang<sup>ab</sup>, Bo Yang<sup>ab</sup>, Weijun Peng<sup>a</sup>, Xingui Xiong<sup>ab\*</sup>

### ABSTRACT

Rheumatoid arthritis (RA) is a systemic autoimmune disease characterized by synovial inflammation and hyperplasia. The complexity of pathway networks within RA has not been well defined. To discover the pathway networks that were involved in RA pathological process and investigate the pathogenesis of RA, iTRAQ-based quantitative proteomics was used in a collagen-induced arthritis (CIA) model at days 28 and 42 of RA. The data were analyzed using Ingenuity pathway analysis (IPA) software. 69 proteins were repeatedly identified at both time points (day 28 and 42) in the CIA model. 5 proteins (MMP3, APOE, ASPN, LIFR, SERBP1) showed progressive changes in expression. IPA revealed 14 proteins involved in connective tissue disorders. ACLY, A1BG, CA3, FTH1, and FTL have been found associated with “rheumatic disease” and “arthritis” in CIA model for the first time. LXR/RXR activation in CIA model was first discovered in IPA pathway analysis. Network analysis revealed several focus proteins in the four significant networks. The progressively changed proteins, MMP3, APOE and ASPN, LIFR, SERBP1, may be correlated with RA disease severity and confirmed by WB and IHC. The findings will provide a new range for elucidation of the pathogenesis of RA in the near future.

**Keywords:** Rheumatoid arthritis, Collagen-induced arthritis, iTRAQ-based quantitative proteomics, Ingenuity pathway analysis

### Introduction

Rheumatoid arthritis (RA) is a chronic, systemic autoimmune inflammatory disorder characterized by inflammation and by destruction of cartilage and bone tissue within synovial joints. RA can cause joint destruction and functional disability if not adequately treated. The exact cause of RA is not fully understood; however, novel cytokines and mediators, being linked to RA pathogenesis, act as bridges to understand the complex pathobiological mechanisms underlying RA.<sup>1-3</sup> In fact, the signaling pathways that contain these cytokines and mediators are increasingly identified in RA onset and progression.<sup>4,5</sup> For example, interleukin-6 (IL-6) activation of the Janus kinase (JAK)/signal transducer and activator of transcription (STAT) pathway is responsible for down-regulation of major cartilage-specific matrix genes<sup>6</sup> and nuclear factor (NF)- $\kappa$ B signaling controls the expression of cytokines IL-1 $\beta$  and tumor necrosis factor (TNF)- $\alpha$ , essential mediators of inflammation in rheumatoid arthritis. Research has shown that inhibitors of NF- $\kappa$ B reduced arthritis severity in several animal

<sup>a</sup> Institute of Integrated Medicine, Xiangya Hospital, Central South University, No. 87 Xiangya Road, Changsha, 410008, China.. E-mail address: xiongxg07@gmail.com. Fax: +86-731-84327568; Tel: +86-731-84327569.

<sup>b</sup> Key Laboratory of Chinese Gan of State Administration of Traditional Chinese Medicine, Changsha, 410008, China.

<sup>c</sup> Central of Telemedicine, Xiangya Hospital, Central South University, No. 87 Xiangya Road, Changsha, 410008, P R China.

<sup>d</sup> Institute of Integrated Medicine, the first affiliated hospital of Soochow university, No.188 Shizi Street, Soochow, Jiangsu, 215006, China.

<sup>e</sup> Department of Pathology & Immunology, Baylor College of Medicine, Baylor College of Medicine One Baylor Plaza, BCM 315, Houston, 77030, US.

† Electronic supplementary information (ESI) available.

models of arthritis.<sup>7,8</sup> Unfortunately, the complex mechanisms of RA makes it difficult to determine the full range of interactions between the molecules and pathways involved in RA. Thus, treatments that target only one protein or pathway may not be very effective and can't better understand pathogenesis of RA. So we should develop an understanding of proteins within the complex RA pathways.

Collagen-induced arthritis (CIA) in rats is a well-established model with many similarities to RA and is widely used to investigate the pathogenesis of RA. This model elicits an immune response in the joints, which is characterized by severe inflammation and cellular infiltration of synovial tissue and damage to cartilage and bone. The histopathological changes similar to those observed in human RA.<sup>9</sup>

Recent advances in proteomics provide an impetus for study the pathological mechanisms, disease progression, or drug treat. In a previous proteomic study, in the SF of patients with RA, the expression of S100A8, S100A9 and S100A12 proteins was higher than those in patients with osteoarthritis (OA) and other miscellaneous inflammatory arthritis.<sup>10</sup> In another proteomic study, the expression of 6 vasculature development-related proteins were up-regulated, while 11 redox-related proteins were down-regulated in RA patients compared to normal.<sup>11</sup> An immunoproteomics analysis of synovial fluid from RA and OA patients conducted by Biswas *et al.*, has been reported to identify autoantigens in RA.<sup>12</sup> Lorenz P et al analyzed the joints of CIA rats using two-dimensional (2-DE) gel-based proteomics and identified 76 spots.<sup>13</sup> However, the widely recognized limitation of 2-DE, such as lacks of repetition, limited range of protein separation and difficulty in combined with mass spectrometer, has restricted the further application. In recent years, quantitative proteomic techniques that couple the use of isobaric tags for relative and absolute quantification (iTRAQ) with strong cation exchange (SCX)-reverse phase liquid chromatography-tandem mass spectrometry (SCX-LC MS/MS) has been developed. In iTRAQ, protein tagging occurs on primary amines allowing for the tagging of most tryptic peptides. Additionally, multiplexing is possible with iTRAQ, which is available in four to eight different tags, and allows us to simultaneously compare proteins at different time points. Ingenuity Pathway Analysis (IPA) is a leading provider with broad range of flexible solutions for the exploration, interpretation, and analysis of the complicated experiment datasets and are used by hundreds of leading scientific research institution worldwide, including pharmaceutical, biotechnology, and academic institutions.<sup>14-16</sup> iTRAQ-based quantitative proteomics combined with IPA analysis offers a deeper biological understanding of molecular and cellular mechanisms of RA on multiple levels and is an important step towards understanding RA pathogenesis.

In the present study, we used iTRAQ-based quantitative proteomics to identify differentially expressed proteins (DEPs) in synovial tissue from different time points in CIA rats. Ingenuity pathway analysis (IPA) was used to analyze the biological functions, pathways, and interaction networks associated with these DEPs. Western blotting and immunohistochemical (IHC) analyses were used to confirm the presence of select proteins. This research could lead to an better understanding of pathogenic mechanisms by analyzing the DEPS and the involved functions, pathways, and interaction networks in a rat model of CIA. The key molecules of the networks found in this study has the potential to become molecular targets. These data will be exploited to elucidate the pathogenesis of RA in the future.

## Materials and methods

### Animals

Healthy Sprague Dawley rats (n=120, 6–7 weeks old, 180 ± 200 g), clean grade, equal males and females, were provided by the animal experimental center of Hunan People's Hospital (Hunan, China). All rats were housed five per cage and received food and water ad libitum under controlled environmental conditions (room temperature 20°C ± 3°C, room humidity 40–60%, background noise 40 ± 10 db, 12:12-h light-dark cycles) for 1 week to adapt to the environment. The 120 rats were divided into the control group and the experimental group at random (40 in the control group, 80 in the experimental group). The study was verified and approved by the Animal Ethics Committee of Hunan People's Hospital and performed in accordance with the Hunan People's Hospital guidelines for the care and use of laboratory animals.

### Induction and assessment of CIA

CIA was initiated according to the protocol for the successful induction in Rats. Briefly, bovine type II collagen (B $\square$ C, 2mg/ml, Chondrex, Inc. Immunization) was mixed with acetic acid followed by complete Freund's adjuvant (CFA, 1mg/ml, Sigma-Aldrich). On day 0, the rats were injected intradermally at the base of the tail with 200- $\mu$ g of the collagen/CFA emulsion for primary immunization. On day 7, the rats were given 100- $\mu$ g of collagen/incomplete Freund's adjuvant (IFA, 1mg/ml, Sigma-Aldrich) emulsion for secondary immunization in the same manner. Eighty CIA rats were divided randomly into two groups, CIA at day 28 (CD 28, n=40) and CIA at day 42 (CD 42, n=40). The normal control group receive no treatment.

The rats were clinically assessed and paw measurements were recorded after disease onset. According to the clinical scoring system [9], hind foot arthritis severity was scored on a scale of 0–3, where 0= no inflammation, 1= inflammation of the ankle joint, 2= inflammation of the foot pad, and 3= inflammation of one or more digits. The disease score of hind limbs was calculated for each animal (maximum score 6 per rat). The thickness of each hind paw was measured with a compass and millimeter ruler in the fixed position after immunization; body weight was monitored throughout the study.

For detection of serum inflammatory cytokines, blood was drawn on days 28 and 42 postimmunization (5 samples each), stored at room temperature for 2 hours, and centrifuged at 1000 r/min for 15 minutes. The serum was added to an ELISA kit (Wuhan Huamei Biotech Co., LTD) to detect the levels of IL-1 $\beta$  and TNF- $\alpha$ .

Hind paws were removed 14, 28, and 42 days after primary immunization for histological assessment (5 samples each). Briefly, the paws were fixed in 10% neutral formalin for 24 hours, decalcified in 14% EDTA fluid for 5 days, neutralized in 5% sodium thiosulfate for 3 hours, and embedded in dehydrate paraffin. Longitudinal sections (5–6 $\mu$ m) were cut from the center of the ankle joint, baked in a 60°C oven for 30 minutes, and stained with hematoxylin and eosin (H&E). Sections were observed by light microscope (CX21; Olympus, Tokyo, Japan) for pathological changes.

All animals were measured before immunization and the data were included as normal control group of animals.

### Tissue preparation and protein extraction

Synovial tissue was isolated from the hind paws of CD28 and CD42 and the normal controls (NC) rats (10 samples each). To extract proteins, the tissue was dissolved in lysis buffer (8 M urea, 4% chaps, 30 mM HEPES, 1 mM PMSF, 2mM EDTA, and 10 mM DTT) at 4°C for 1h, placed in ultrasound (water

bath, 5 minutes), and then centrifuged at 20,000 rpm for 25 minutes. The supernatant was collected and DTT was added to a final concentration of 10 mM. The resulting solution was incubated in a water-bath at 56°C for 1 hour followed by quick addition of iodoacetamide to a final concentration of 55 mM. Then leave the solution stand in a dark room for 1 hour with room temperature 20-25°C. The protein samples were precipitated (-20°C, 3 hours) by addition of precooled acetone and then centrifuged (20,000 × g, 20 minutes, 4°C). The proteins were solubilized in 0.5M triethylammonium bicarbonate plus 0.1% sodium dodecyl sulfate (SDS). Protein concentration was determined with a Bradford protein assay kit (Amesco). To diminish the effect of sample inherent biological variation on the results of a proteomics analysis, equal amounts of protein from each of the 10 synovial tissue samples were pooled to generate one common sample, as described in previous research.<sup>17</sup>

### iTRAQ method

Trypsin digestion and iTRAQ labeling were performed according to the manufacturer's protocol (Applied Biosystems). Briefly, 100 µg of protein from each pooled sample was reduced, alkylated, and then digested overnight at 37°C with trypsin. A sample (1 µL) of the tryptic peptides was taken to detect digestion efficiency using Ultraflex TOF/TOF (Bruker, Germany). The tryptic peptide solution of each sample was labeled with iTRAQ reagents according to the iTRAQ Reagent Multiplex Kit protocol (Applied Biosystems). We used 8-plex kit for differential labeling. Normal control, CD 28 and CD 42 derived tryptic peptides were labeled with 113, 114 and 115, respectively. The tryptic peptide samples were labeled, mixed and dried before further analyses. We calculated the labeling efficiency, as described in previous researches,<sup>18</sup> the total number of possible labeling sites (the N-termini of all peptides and lysine side chains) for iTRAQ tags were compared with the labeled sites in the detected peptides. The iTRAQ peptide labeling efficiency was more than 97% in this study.

The mixed peptides were fractionated on a SCX column (Luna SCX 100A, phenomenex). The mixed iTRAQ-labeled sample was diluted with 10× buffer A (25% acetone (ACN), 10mM KH<sub>2</sub>PO<sub>4</sub>, pH 3.0). Buffer B was identical to buffer A except it contained 2M KCl. SCX fractionation was performed using a linear binary gradient of 0–100% buffer B in buffer A at a flow rate of 1 mL/min. Based on the SCX chromatograms, 10 SCX fractions were collected along the gradient. Each SCX fraction was dried, dissolved in buffer C (5% ACN, 0.1% FA), and analyzed on a reverse-phase liquid chromatography column (Strata-X C18 column, 5µm, 300A, 100mm×75mm, Phenomenex). The HPLC gradient was increased from 5% to 30% in 65 minutes at a flow rate of 400 nl/min. Mass spectrometric analysis of the iTRAQ-labeled samples was performed on Q Exactive LC-MS/MS (Thermo Scientific Co.). Sequences for the peptide and reporter ions were generated to identify the protein from which the peptide originated. To diminish the effect of experimental variation, three independent MS/MS runs were performed for each sample.<sup>19</sup>

Proteome Discoverer Software (Thermo Scientific version 1.3) was used for data acquisition and quantification. Data sifted by Proteome Discoverer were used to identify proteins with Mascot (version 2.3.0, Matrix Science, London, UK) and the Uniprot-rat database (<http://www.uniprot.org/>). Mascot search parameters used included trypsin, peptides digested with a maximum of one missed cleavage, fixed modification (carbamidomethylation of cysteine residue), variable modifications (oxidation of methionine Gln-Pyro-Glu of N-term Q, and iTRAQ 8 plex modification of N terminal, K and Y), peptide tolerance 15 ppm, and the iTRAQ fragment tolerance (0.2 Da). Using these criteria 59,285 spectra were identified with 95% confidence. The quantitative result of the peptide was the ratio of the

signal intensity value of the reference sample (normal sample) label to the signal strength values of other labels. Protein quantitative ratio was calculated as the median of all peptide ratios. The final quantitative result was normalized to the median ratio of each label. The fold change of differentially expressed proteins was calculated as the average value from the protein iTRAQ ratios. The DEPs were identified with the following criteria:  $\geq 2$  peptide matches, proteins repeatedly identified in three replications, and those with an average ratio-fold change  $\geq 1.3$  or  $\leq 0.77$  between the groups and p value  $< 0.5$ .

### **Bioinformatics analyses of DEPs**

IPA was used to analyze biological functions, pathways, and networks associated with the identified DEPs. The data packet containing protein IDs from the Uniport-rat database and corresponding abundance changes was uploaded into IPA. Each identifier was mapped to the corresponding molecule in the Ingenuity Pathway Knowledge Base. A detailed description of IPA analysis is available at Ingenuity System's web site (<http://www.ingenuity.com>). IPA analysis identified "immune disease" as the main disease associated with the differentially expressed proteins by biological function.

### **Western blotting**

Western blotting was performed for select proteins identified by iTRAQ in NC, CD28, and CD42 (10 samples each). Protein samples (30–50  $\mu\text{g}$ ) were separated by 12% SDS-polyacrylamide gel electrophoresis and then transferred onto polyvinylidene difluoride membranes (Bio-Rad). Following blocking with 5% skim milk, the transferred membranes were incubated overnight at 4°C with primary anti-isoform 2 of plasminogen activator inhibitor 1 RNA-binding protein (SERBP1) antibody (1:1000; Abcam), anti-matrix metalloproteinase-3 (MMP3) antibody (1:200; Santa cruz), anti-apolipoprotein E (APOE) antibody (1:200; Santa cruz), anti-asporin (ASPN) antibody (1:200; Santa cruz), and anti-leukemia inhibitory factor receptor (LIFR) antibody (1:500; Santa cruz). The membranes were subsequently incubated with horseradish peroxidase-conjugated secondary antibodies (1:3000; Proteintech) for 1 hour at room temperature. Bands were visualized with an electrochemiluminescence detection reagent (Thermo Scientific Pierce) and quantified by densitometry using the Image-Quant image analysis system (Storm Optical Scanner, Molecular Dynamics).  $\beta$ -actin was detected simultaneously as a loading control. All Western blot analyses were performed in triplicate.

### **Immunohistochemistry**

IHC was performed to confirm expression levels of select proteins identified by iTRAQ in NC, CD28, and CD42 (10 samples for each). Briefly, serial sections (4  $\mu\text{m}$ ) were cut, rehydrated, and treated with an antigen retrieval solution (10 mmol/L sodium citrate buffer, pH 6.0). Endogenous peroxidase was blocked using 3% hydrogen peroxide in methanol for 20 min. Nonspecific sites were blocked for 20 minutes using 1% normal serum in phosphate buffered saline. IHC was performed using the same antibodies with Western blotting. The sections were incubated overnight at 4°C with anti-SERBP1 (dilution 1:100), anti-MMP3 (dilution 1:100), anti-APOE (dilution 1:100), anti-ASPN (dilution 1:50) and anti-LIFR (dilution 1:100). The sections were then incubated in a 1:1000 dilution of biotinylated secondary antibody followed by avidin-biotin peroxidase complex (DAKO) according to the manufacturer's instructions. The tissue sections were incubated with 3,3-diaminobenzidine (Sigma) until a brown color developed and counterstained with hematoxylin. For the negative controls, the

primary antibodies were omitted. Immunostaining was blindly evaluated by two investigators in an effort to provide consensus on staining patterns.

**Statistical analyses** SPSS software (IBM, v19) software was used for statistical analyses. The data were expressed as means  $\pm$  SD. Group comparisons were performed by the analysis of two-way repeated-measures analysis of variance and two tailed independent t test. A value of  $P < 0.05$  was considered statistically significant.

## Results

### CIA rat information

As expected, the CIA group developed arthritis. As previously reported,<sup>20</sup> clinical signs of arthritis, including clinical scores (Fig. 1A), paw swelling (Fig. 1B), weight changes (Fig. 1C), and high expression of inflammatory cytokines (TNF- $\alpha$  and IL-1  $\beta$ ) developed. The first signs of arthritis were evident between days 7 and 14 postimmunization. As shown in Fig.1A, there was a significant difference in the clinical scores of the two groups at day 7. However the most significant change in clinical scores was observed on day 21. A significant change in paw swelling was observed on day 7 and was exacerbated throughout the time course of CIA in the rat (Fig. 1B). The CIA group showed a significant weight reduction compared with the control group (Fig. 1C). IL-1 $\beta$  and TNF- $\alpha$  serum levels increased progressively in the CIA day group 42 versus the day 28 group; both of which were increased compared to the control group (Fig. 1D). Histological examination of ankle sections from days 14, 28, and 42 postimmunization revealed inflammatory cell infiltration, synovial thickening, and joint degradation. The severity of these characteristics increased with the passage of time (Fig. 1E).

### Identification of DEPs between the control and CIA group

We identified 1695 proteins with a false discovery rate (FDR) of 1% and unique peptide matches  $\geq 2$ . Of the identified proteins, 1342 were repeatedly identified in triplicate experiments (Fig. 2A). DEPs between the two stages (CD28/NC, CD42/NC, and CD42/CD28) were compared by the criteria ( $\geq 1.3$  or  $\leq 0.77$ ) as described above. In CD28, 65 and 41 proteins were found to be over- and under-expressed, respectively, and, in CD42, 90 and 49 proteins were found to be over- and under-expressed, respectively, compared to the control group (see ESI†). Of the differentially expressed proteins, 45 and 24 remained over- and under-expressed, respectively, at both time points (day 28 and 42) (Fig. 2B). The names of these 69 proteins and the stages at which their expression was significantly altered are shown in Table 1. Among these differential proteins, four proteins (MMP3, APOE, ASPN, and LIFR) showed progressive up-regulated and one proteins (SERBP1) were progressively down-regulated at days 42 and 28 in the CIA rats versus the controls (Table 1, shown in bold). Most of these proteins have been previously reported as being associated with RA.<sup>21-26</sup> MS/MS spectra used for the identification and quantitation of SERBP1, MMP3, APOE ASPN and LIFR are shown in ESI†.

### Bioinformatic analysis of the DEPs

The 69 differentially expressed proteins were imported into IPA software for biological functions, canonical pathways, and significant networks analysis. IPA functional analysis contains three primary categories of functions: diseases and disorders, molecular and cellular functions, and physiological

system development and function. The biological functions were shown in ESI†. Connective tissue disorders category was found to be the most significant, which consist of A1BG, ACLY, APOE, ASPN, BGN, COL9A1, FN1, FTH1, FTL, LUM, MMP3, SPARC, COL5A2, CA3 (Fig. 3 and see ESI†). This result indicated that connective tissue disorders related proteins were specifically regulated in CIA rats synovial tissues.

Of the diseases listed in the connective tissue disorders category, “rheumatic disease” was found to be the most significant ( $P = 4.61E-07$ ) disease annotation. It should be noted that the diseases annotation “arthritis” also with higher significance and activated. This two category shared several proteins, including APOE, ASPN, BGN, COL9A1, FN1, LUM, and MMP3 (Table 2).

Based on the 69 DEPs proteins, IPA canonical pathways analysis identified 68 canonical pathways (see ESI†). Twenty two canonical pathways were significantly perturbed with  $p < 0.05$ , which corresponds to  $-\log(p\text{-value}) > 1.3$  identified by the IPA (Fig. 4). LXR/RXR activation was found to be the most significant ( $-\log(p\text{-value}) = 5.04$ ) and five proteins (APOE, HPX, ITIH4, ACACA, A1BG) involved in this pathway (Fig. 4 and see ESI†).

We systematically evaluated the functions of identified proteins by investigating the results of network analysis. IPA interaction analysis found 4 significant networks (Table 3 and Fig. 5). 25 proteins involved in cell-to-cell signaling and interaction, connective tissue disorders, and inflammatory disease were grouped as the top #1 network (IPA score 46, Fig. 5A). APOE and MMP3 which have been previously reported to be associated with rheumatic disease,<sup>22,27</sup> play key roles in this network. In addition to proteins identified in our study as differentially expressed, other proteins such as transforming growth factor- $\beta$ 1 (TGF- $\beta$ ), IL-1, and ERK1/2 from Network 1 and TGF-B1 and UBC from Network 2 play central roles in these networks.

### Validation of DEPs

Five proteins (SERBP1, MMP3, APOE ASPN and LIFR) were chosen for further expression validation of alterations. MMP3, APOE ASPN and LIFR was found to be up-regulated in CIA rats at days 28 (with fold change 1.31, 1.35 1.39 and 1.46 respectively) and then up-regulated progressively at days 42 (with fold change 1.79, 1.80 1.92 and 2.35 respectively), whereas SERBP1 was found to be down-regulated progressively (with fold change 0.63 at days 28 and 0.49 at days 42) by iTRAQ quantitation in our study.

Western blotting was performed to detect expression of SERBP1, MMP3, APOE ASPN and LIFR in the synovial tissue of CIA rats at days 28 and 42, and in the normal control. As shown in Fig. 6A, MMP3, APOE ASPN and LIFR were progressively up-regulated and SERBP1 was progressively down-regulated in the CIA versus NC. This was consistent with the findings of iTRAQ.

IHC was used to detect the expression of SERBP1, MMP3, APOE ASPN and LIFR in an independent set of synovial tissues from CIA28, CIA42, and the NC. A representative IHC image is shown in Fig. 6B, MMP3, APOE ASPN and LIFR showed strong immunostaining in the synovial tissues of CIA28 and 42, whereas these proteins displayed weak staining in the NC. Moreover, the staining was stronger in CIA42 than in CIA28. SERBP1 showed strong immunostaining in synovial tissue of the NC, whereas it showed weak staining in CIA28 and 42. Furthermore, the staining was weaker in CIA42 than in CIA28. The IHC results also confirmed the iTRAQ-based quantitative proteomics findings, which suggested that the proteomic analyses based on iTRAQ were convincing.

## Discussion

The pathogenic mechanism of RA remains unclear.<sup>28</sup> Although animal models may not reproduce all of the features of human RA, CIA in rats has several common immunological and pathological features and this model can help us to understand the normal inflammatory and immune responses that occur during RA pathogenesis.<sup>9,29</sup> In this study, we demonstrated that CIA rats represent obvious clinical signs of arthritis, elevated inflammatory cytokine levels, and typical histopathological features, which are in accordance with previous studies.<sup>30</sup>

Identification of proteins with altered expression in RA versus normal joints could provide valuable insight into proteins that contribute to synovial inflammation. In this study, iTRAQ-based quantitative proteomics was used to identify DEPs during synovial pathogenesis. The 69 identified proteins were associated with multiple IPA biological categories related to RA. In the bio-function analysis, connective tissue disorders; inflammatory disease; skeletal and muscular disorders and connective tissue development and function are found to be intimately associated with RA. Connective tissue disorders category which contains 14 proteins was found with the highest significance. Several proteins were well known for their close links with connective tissue, such as collagen, type IX, alpha 1 (COL9A1), collagen, type V, alpha 2 (COL5A2), and secreted protein, acidic, cysteine-rich (SPARC). Another several proteins of the 14 proteins were previously reported to be associated with rheumatic disease. Biglycan (BGN) is a secreted proteoglycan that found in articular cartilage, has been reported that interact with ECM components including growth factors and cytokines, such as TGF- $\beta$ , TNF- $\alpha$ , and IL-1<sup>31</sup> and play a crucial role in the regulation of inflammation.<sup>32,33</sup> One study showed that patients with RA expressed a significantly higher immunity to small proteoglycans biglycan than in OA.<sup>34</sup> Fibronectin (FN) is a multifunctional, ECM glycoprotein. Research has shown that citrullinated FN can be detected in rheumatoid synovial tissue and synovial fluid and it may be involved in the pathogenesis of RA by modulating inflammation, inhibiting apoptosis, pannus invasion, and other events associated with RA progression.<sup>35,36</sup> Lumican (LUM), a SLRP found in the ECM, is a major proteoglycan component that binds to collagen in bone and its secretion reflects bone repair.<sup>37</sup> LUM has been shown to promote secretion of pro-inflammatory cytokines<sup>38</sup> and is overexpressed in the synovial fluid of RA patients.<sup>39</sup>

Interestingly, five of these 14 proteins associated with connective tissue disorders in this study seldom reported to be associated with RA. ATP citrate lyase (ACLY) is an enzyme responsible for the synthesis of fatty acid. Alpha-1B-glycoprotein (A1BG) is known as a member of immunoglobulin supergene family and may be associated with innate immunity and cell adhesion. It has been detected in osteoarthritic knee synovial fluids by 2-dimensional gel electrophoresis(2-DE) technique, however, its function is still uncertain.<sup>40,41</sup> Both ferritin heavy polypeptide 1(FTH1) and ferritin light chain 1(FTL) are responsible for intercellular iron storage and have been shown to alleviate oxidative damage.<sup>42,43</sup> Moreover, FTL plays an anti-inflammatory role in response to LPS in murine macrophages.<sup>44</sup> Carbonic anhydrase 3 (CA3) was expressed at higher levels in skeletal muscle and much evidence has shown that carbonic anhydrase inhibitors can restrain bone resorption.<sup>45</sup> In this study, ACLY, A1BG, CA3, FTH1, and FTL have been found associated with “rheumatic disease” and “arthritis” in the CIA model for the first time, which may provide clues to further study the roles of these proteins in the RA pathological process.

Canonical pathway analysis revealed 68 pathways associated with the dataset. Liver X receptor/retinoid X receptor (LXR/RXR) activation was found to be the most significant. LXR, a members of nuclear receptors, function as heterodimers with RXR. Previous study indicate that LXR involved in

cholesterol and lipid metabolism and orchestrated inflammatory response through inhibit inflammatory mediators expression which stimulated by LPS, TNF- $\alpha$  and (IL)-1 $\beta$ .<sup>46,47</sup> The activation of LXR/RXR inhibits LPS-induced inflammatory responses in the central nervous system.<sup>48</sup> However, the role of LXR/RXR activation in RA has not been reported. LXR/RXR activation was first discovered and APOE, HPX, ITIH4, ACACA, A1BG were found to be involved in this pathway in this study. LXR/RXR-related inflammatory may be a potential mechanism in the pathogenesis of CIA rats.

Network analysis revealed that the top-ranked networks of differentially expressed proteins were tightly associated with connective tissue disorders and inflammatory disease. The analysis has identified several focus hubs (e.g., TGF- $\beta$ , IL-1, ERK1/2, VEGF, and p38 MAPK) with high degree of interactions. It is well known that the process of RA involves an chronic inflammatory disorder. These focus hubs are involved in the inflammation response to RA which have been validated that inflammation is the key mechanisms for RA.<sup>49</sup> In this study, we also revealed that several focus proteins (APOE, MMP3, SERBP1, BGN, LIFR, FN1, and ATP1B1) play key roles in four significant networks. The levels of these protein were affected by numerous inflammatory cytokines including IL-1 and TGF-B, However, the complex interactions between different signaling pathways requires further study.

In this study, we also found that 5 proteins (MMP3, APOE, ASPN, LIFR, and SERBP1) of the 69 identified proteins showed progressive changes in expression at days 28 and 42 compared to the NC synovial tissue samples and were selectively validated. The five proteins have been previously reported as being associated with RA. The progressive changes suggest the expression of these proteins maybe correlated with RA disease severity.

SERBP1, also called PAI-RBP1, was named for its interaction with plasminogen activator inhibitor type 1 (PAI-1) and plays a role in PAI-1 mRNA stability.<sup>25</sup> PAI-1 is an inhibitor of plasmin production. Plasmin can directly degrade extracellular matrix components and the basement membrane or it can indirectly contribute to cartilage and bone matrix degradation by activating MMPs and proteoglycanases. Plasmin also induces cytokine expression in monocytes.<sup>26</sup> In this study, SERBP1 was found to be down-regulated progressively suggest that the gradually decreasing inhibition of PAI-1 result in increasing cartilage and bone destruction during CIA pathology.

MMP3 belongs to the MMP family whose members are involved in extracellular matrix (ECM) breakdown and act as mediators of cartilage and bone matrix degradation in RA.<sup>50</sup> MMP-3 is present in RA synovial fluid and overexpressed in rheumatoid synovial tissue.<sup>27</sup> Accumulating evidence indicates that MMP-3 plays an important role in RA pathology and it is considered to be an important protease in joint damage where it cleaves a series of ECM proteins.<sup>51</sup> The active form of MMP-3 is a key enzyme involved in RA-associated destruction of cartilage and bone<sup>21</sup>. Mamehara A et al reports the potential of MMP3 to be a useful marker for prediction of joint destruction.<sup>52</sup> Ma JD et al reported that serum MMP-3 was higher in RA patients with high grade synovitis than that of low grade synovitis and significantly correlated with synovitis score and activation of synovial stroma subscore.<sup>53</sup> The progressive changes of MMP3 in this study indicated that MMP3 is closely related to severity of bone erosion.

APOE is a glycoprotein involved in lipid transport and metabolism. There is increasing evidence to suggest that APOE is strongly linked to immunomodulation, anti-inflammatory, and oxidation<sup>54,55</sup> and impact ECM remodeling.<sup>56</sup> A recent study revealed that APOE knockout mice developed exacerbated CIA, which indicated that Apo E might play a role in RA. Another study also supported the role of Apo E in the the pathophysiology of arthritis. However, it reported that Apo E-deficient

mice are resistant to the development of CIA.<sup>57</sup> The results observed in the two study are clearly contradictory. The reason for these inconsistency may be due to the use of different CIA models<sup>22</sup> In this study, the expression of APOE was progressively up-regulated suggest that the high expression of APOE is closely associated with exacerbated CIA.

Asporin (ASPN) belongs to a family of SLRPs associated with the cartilage matrix. Although SLRPs play roles in skeletal growth, craniofacial structure, and collagen fibrillogenesis are well known,<sup>58</sup> the exact role of ASPN is not known. A correlation between ASPN and RA by the observations made by Torres B, who reported that asporin D repeat polymorphism is unrelated to the susceptibility to RA, however, it may influence the outcome of the disease.<sup>59</sup> Kizawa et al reported that ASPN is over-expressed in OA articular cartilage, and the expression increases with progressive cartilage degeneration.<sup>60</sup> A role for ASPN in the pathology of osteoarthritis is further supported by the observations made by Sakao and coworkers, who reported that increased ASPN expression was significantly associated with the severity of cartilage degeneration.<sup>61</sup> In this study, ASPN was found to be up-regulated progressively suggests that ASPN may play the similar role in the development of CIA, which may provide clues as to the underlying pathology of CIA.

LIFR, also called glycoprotein-190 (gp 190), is a subunit of a receptor for LIF. LIF stimulates the proliferation and differentiation of both osteoblasts and osteoclasts and regulates bone formation and bone resorption, which was associated with RA pathogenesis.<sup>62</sup> LIF stimulates osteoclast formation by enhancing the expression of receptor activator of nuclear factor kappa-B ligand (RANKL), which is the primary mediator of osteoclast formation, function, and survival. Increased levels of LIF have been detected in RA synovial fluids and tissues<sup>24</sup>. The progressive changes of LIFR in this study suggest that LIFR may play an important role in bone cartilage degeneration in CIA rats.

## Conclusions

In summary, we demonstrate the feasibility of using iTRAQ-based quantitative proteomics to identify DEPs in CIA rats versus normal controls. Of the identified proteins, five proteins(MMP3, APOE, ASPN, LIFR, and SERBP1) showed progressive changes in expression which suggest the correlation with RA disease severity. Ingenuity pathway analysis revealed multiple biological functions associated with RA and 14 proteins were found to be involved in connective tissue disorders. ACLY, A1BG, CA3, FTH1, and FTL have been found associated with “rheumatic disease” and “arthritis” in CIA model for the first time. LXR/RXR activation in CIA rats was first discovered as the top enriched pathways in this study and LXR/RXR-mediated inflammatory reaction may be a potential pathogenic mechanism of CIA rats. Network analysis revealed that APOE, MMP3, SERBP1, BGN, LIFR, FN1, and ATP1B1 play key roles in four significant networks. WB and IHC results confirmed the iTRAQ-based quantitative proteomics findings. The findings will provide a new range for elucidation of the pathogenesis of RA in the near future. Further functional study for elucidating the regulatory roles of these proteins would greatly improve our understanding of the complex molecular mechanisms in CIA rats.

## Competing interests

We declare that all authors agree with the content of the submitted manuscript and that there are no conflicts of interest.

## Acknowledgments

This work was funded by a grant from the National Natural Science Foundation of China (81102564,81303098), Specialized Research Fund for the Doctoral Program of Higher Education (20110162120004), Traditional Chinese Medicine Scientific Research Project of Hunan Province (201003), Key-discipline Construct Programs of Hunan Province and the State Administration of Traditional Chinese Medicine.

## References

- 1 Y. Tanaka. *Nihon Rinsho.*, **2013**,71,1147-1152.
- 2 Y. Hou, H. Lin, L. Zhu, Z. Liu, F. Hu, J. Shi, T. Yang, X. Shi, M. Zhu, B. F. Godley, Q. Wang, Z. Liand Y. Zhao. *Arthritis Rheum.*, **2013**,65,2835-2846.
- 3 E. J. Nam, J. H. Kang, S. Sung, K. H. Sa, K. H. Kim, J. S. Seo, J. H. Kim, S. W. Han, I. S. Kimand Y. M. Kang. *Arthritis Rheum.*, **2013**,65,1753-1763.
- 4 V. Romero, J. Fert-Bober, P. A. Nigrovic, E. Darrah, U. J. Haque, D. M. Lee, van Eyk J, A. Rosenand F. Andrade. *Sci Transl Med.*, **2013**,5,209ra150.
- 5 G. D. Kalliolias, B. Zhao, A. Triantafyllopoulou, K. H. Park-Minand L. B. Ivashkiv. *Arthritis Rheum.*, **2010**,62,402-413.
- 6 F. Legendre, J. Dudhia, J. P. Pujoland P. Bogdanowicz. *J. Biol. Chem.*, **2003**,278,2903-2912.
- 7 S. S. Makarov. *Arthritis Res.*, **2001**,3,200-206.
- 8 T. Tomita, E. Takeuchi, N. Tomita, R. Morishita, M. Kaneko, K. Yamamoto, T. Nakase, H. Seki, K. Kato, Y. Kanedaand T. Ochi. *Arthritis Rheum.*, **1999**,42,2532-2542.
- 9 J. A. Luross, N. A. Williams. *Immunology.*, **2001**,103,407-416.
- 10 A. Baillet, C. Trocme, S. Berthier, M. Arlotto, L. Grange, J. Chenau, S. Quetant, M. Seve, F. Berger, R. Juvin, F. Moreland P. Gaudin. *Rheumatology (Oxford).*, **2010**,49,671-682.
- 11 J. G. Wang, W. D. Xu, W. T. Zhai, Y. Li, J. W. Hu, B. Hu, M. Li, L. Zhang, W. Guo, J. P. Zhang, L. H. Wangand B. H. Jiao. *Arthritis Rheum.*, **2012**,64,993-1004.
- 12 S. Biswas, S. Sharma, A. Saroha, D. S. Bhakuni, R. Malhotra, M. Zahur, M. Oellerich, H. R. Dasand A. R. Asif. *PLoS One.*, **2013**,8,e56246.
- 13 P. Lorenz, M. Bantscheff, S. M. Ibrahim, H. J. Thiesenand M. O. Glocker. *Clin. Chem. Lab. Med.*, **2003**,41,1622-1632.
- 14 J. Frobel, R. P. Cadeddu, S. Hartwig, I. Bruns, C. M. Wilk, A. Kundgen, J. C. Fischer, T. Schroeder, U. G. Steidl, U. Germing, S. Lehr, R. Haasand A. Czibere. *Mol. Cell Proteomics.*, **2013**,12,1272-1280.
- 15 D. J. Coble, D. Fleming, M. E. Persia, C. M. Ashwell, M. F. Rothschild, C. J. Schmidtand S. J. Lamont. *BMC Genomics.*, **2014**,15,1084.
- 16 A. G. Uren, J. Kool, K. Matentzoglou, de Ridder J, J. Mattison, van Uitert M, W. Lagcher, D. Sie, E. Tanger, T. Cox, M. Reinders, T. J. Hubbard, J. Rogers, J. Jonkers, L. Wessels, D. J. Adams, van Lohuizen Mand A. Berns. *Cell.*, **2008**,133,727-741.
- 17 G. Q. Zeng, P. F. Zhang, X. Deng, F. L. Yu, C. Li, Y. Xu, H. Yi, M. Y. Li, R. Hu, J. H. Zuo, X. H. Li, X. X. Wan, J. Q. Qu, Q. Y. He, J. H. Li, X. Ye, Y. Chen, J. Y. Liand Z. Q. Xiao. *Mol. Cell Proteomics.*, **2012**,11,M111.013946.
- 18 J. Jin, J. Park, K. Kim, Y. Kang, S. G. Park, J. H. Kim, K. S. Park, H. Junand Y. Kim. *J. Proteome Res.*,

- 2009,8,1393-1403.
- 19 D. Ikeda, H. Ageta, K. Tsuchida and H. Yamada. *Biomarkers.*, **2013**,18,565-572.
- 20 A. K. Clark, J. Grist, A. Al-Kashi, M. Perretti and M. M. Malcangio. *Arthritis Rheum.*, **2012**,64,2038-2047.
- 21 A. Lee, S. J. Choi, K. Park, J. W. Park, K. Kim, K. Choi, S. Y. Yoon and I. Youn. *Bioconj. Chem.*, **2013**,24,1068-1074.
- 22 J. Postigo, F. Genre, M. Iglesias, M. Fernandez-Rey, L. Buelta, R. J. Carlos, J. Merino and R. Merino. *Arthritis Rheum.*, **2011**,63,971-980.
- 23 X. Y. Song, M. Gu, W. W. Jin, D. M. Klinman and S. M. Wahl. *J. Clin. Invest.*, **1998**,101,2615-2621.
- 24 H. Okamoto, M. Yamamura, Y. Morita, S. Harada, H. Makino and Z. Ota. *Arthritis Rheum.*, **1997**,40,1096-1105.
- 25 J. H. Heaton, W. M. Dlakic, M. Dlakic and T. D. Gelehrter. *J. Biol. Chem.*, **2001**,276,3341-3347.
- 26 M. O. Judex, B. M. Mueller. *Am. J. Pathol.*, **2005**,166,645-647.
- 27 Y. Akamine, K. Kakudo, M. Kondo, K. Ota, Y. Muroi, H. Yoshikawa and K. Nakata. *Int. J. Oral Maxillofac. Surg.*, **2012**,41,874-881.
- 28 S. A. Yoo, H. J. Yoon, H. S. Kim, C. B. Chae, De Falco S, C. S. Cho and W. U. Kim. *Arthritis Rheum.*, **2009**,60,345-354.
- 29 A. C. Horsfall, D. M. Butler, L. Marinova, P. J. Warden, R. O. Williams, R. N. Maini and M. Feldmann. *J. Immunol.*, **1997**,159,5687-5696.
- 30 S. W. Lee, J. H. Kim, M. C. Park, Y. B. Park and S. K. Lee. *Scand. J. Rheumatol.*, **2008**,37,260-268.
- 31 L. Schaefer, A. Babelova, E. Kiss, H. J. Hausser, M. Baliova, M. Krzyzankova, G. Marsche, M. F. Young, D. Mihalik, M. Gotte, E. Malle, R. M. Schaefer and H. J. Grone. *J. Clin. Invest.*, **2005**,115,2223-2233.
- 32 K. Moreth, R. Brodbeck, A. Babelova, N. Gretz, T. Spieker, J. Zeng-Brouwers, J. Pfeilschifter, M. F. Young, R. M. Schaefer and L. Schaefer. *J. Clin. Invest.*, **2010**,120,4251-4272.
- 33 P. J. Roughley. *Arthritis Res.*, **2001**,3,342-347.
- 34 A. Polgar, A. Falus, E. Koo, I. Ujfalussy, M. Sesztak, I. Szuts, K. Konrad, L. Hodinka, E. Bene, G. Meszaros, Z. Orutay, E. Farkas, A. Paksy and E. I. Buzas. *Rheumatology (Oxford)*, **2003**,42,522-527.
- 35 L. Fan, Q. Wang, R. Liu, M. Zong, D. He, H. Zhang, Y. Ding and J. Ma. *Arthritis Res. Ther.*, **2012**,14,R266.
- 36 S. Shiozawa, R. Yoshihara, Y. Kuroki, T. Fujita, K. Shiozawa and S. Imura. *Ann. Rheum. Dis.*, **1992**,51,869-873.
- 37 A. Raouf, B. Ganss, C. McMahon, C. Vary, P. J. Roughley and A. Seth. *Matrix Biol.*, **2002**,21,361-367.
- 38 K. Lohr, H. Sardana, S. Lee, F. Wu, D. L. Huso, A. R. Hamad and S. Chakravarti. *Inflamm. Bowel Dis.*, **2012**,18,143-151.
- 39 M. Bhattacharjee, R. Sharma, R. Goel, L. Balakrishnan, S. Renuse, J. Advani, S. T. Gupta, R. Verma, S. M. Pinto, N. R. Sekhar, B. Nair, T. S. Prasad, H. C. Harsha, R. Jois, S. Shankar and A. Pandey. *Clin Proteomics.*, **2013**,10,11.
- 40 D. Sun, Y. Y. Zhao, S. P. Dai, K. Fang, L. Y. Dong and Q. Ding. *Yi Chuan Xue Bao.*, **2002**,29,299-302.
- 41 C. P. Chen, C. C. Hsu, W. L. Yeh, H. C. Lin, S. Y. Hsieh, S. C. Lin, T. T. Chen, M. J. Chen and S. F. Tang. *Proteome Sci.*, **2011**,9,65.
- 42 H. L. Storr, B. Kind, D. A. Parfitt, J. P. Chapple, M. Lorenz, K. Koehler, A. Huebner and A. J. Clark. *Mol. Endocrinol.*, **2009**,23,2086-2094.
- 43 M. A. Baraibar, A. G. Barbeito, B. B. Muhoberac and R. Vidal. *Free Radic. Biol. Med.*, **2012**,52,1692-1697.
- 44 Y. Fan, J. Zhang, L. Cai, S. Wang, C. Liu, Y. Zhang, L. You, Y. Fu, Z. Shi, Z. Yin, L. Luo, Y. Chang and X. Duan. *Biochim. Biophys. Acta.*, **2014**,1843,2775-2783.
- 45 L. Staunton, M. Zwyer, D. Swandulla and K. Ohlendieck. *Int. J. Mol. Med.*, **2012**,30,723-733.
- 46 A. J. Fowler, M. Y. Sheu, M. Schmuth, J. Kao, J. W. Fluhr, L. Rhein, J. L. Collins, T. M. Willson, D. J. Mangelsdorf, P. M. Elias and K. R. Feingold. *J. Invest. Dermatol.*, **2003**,120,246-255.

- 47 S. Ogawa, J. Lozach, C. Benner, G. Pascual, R. K. Tangirala, S. Westin, A. Hoffmann, S. Subramaniam, M. David, M. G. Rosenfeld and C. K. Glass. *Cell.*, **2005**,122,707-721.
- 48 D. J. Mangelsdorf, R. M. Evans. *Cell.*, **1995**,83,841-850.
- 49 M. C. Boissier. *Joint Bone Spine.*, **2011**,78,230-234.
- 50 G. S. Firestein. *Nature.*, **2003**,423,356-361.
- 51 S. Sun, A. C. Bay-Jensen, M. A. Karsdal, A. S. Siebuhr, Q. Zheng, W. P. Maksymowych, T. G. Christiansen and K. Henriksen. *BMC Musculoskelet Disord.*, **2014**,15,93.
- 52 A. Mamehara, T. Sugimoto, D. Sugiyama, S. Morinobu, G. Tsuji, S. Kawano, A. Morinobu and S. Kumagai. *Kobe J. Med. Sci.*, **2010**,56,E98-107.
- 53 J. D. Ma, J. J. Zhou, D. H. Zheng, L. F. Chen, Y. Q. Mo, X. N. Wei, L. J. Yang and L. Dai. *Mediators Inflamm.*, **2014**,2014,179284.
- 54 T. E. Toms, J. P. Smith, V. F. Panoulas, H. Blackmore, K. M. Douglas and G. D. Kitas. *J. Rheumatol.*, **2012**,39,218-225.
- 55 M. T. Maehlen, S. A. Provan, de Rooy DP, van der Helm-van Mil AH, A. Krabben, T. Saxne, E. Lindqvist, A. G. Semb, T. Uhlig, van der Heijde D, I. L. Mero, I. C. Olsen, T. K. Kvien and B. A. Lie. *PLoS One.*, **2013**,8,e60970.
- 56 P. S. Bhattacharjee, T. S. Huq, V. Potter, A. Young, I. R. Davenport, R. Graves, T. K. Mandal, C. Clement, H. E. McFerrin, S. Muniruzzaman, S. K. Ireland and J. M. Hill. *PLoS One.*, **2012**,7,e52152.
- 57 D. L. Asquith, A. M. Miller, A. J. Hueber, F. Y. Liew, N. Sattar and I. B. McInnes. *Arthritis Rheum.*, **2010**,62,472-477.
- 58 R. V. Iozzo. *J. Biol. Chem.*, **1999**,274,18843-18846.
- 59 B. Torres, G. Orozco, J. R. Garcia-Lozano, J. Oliver, O. Fernandez, M. A. Gonzalez-Gay, A. Balsa, A. Garcia, D. Pascual-Salcedo, M. A. Lopez-Nevot, A. Nunez-Roldan, J. Martin and M. F. Gonzalez-Escribano. *Ann. Rheum. Dis.*, **2007**,66,118-120.
- 60 H. Kizawa, I. Kou, A. Iida, A. Sudo, Y. Miyamoto, A. Fukuda, A. Mabuchi, A. Kotani, A. Kawakami, S. Yamamoto, A. Uchida, K. Nakamura, K. Notoya, Y. Nakamura and S. Ikegawa. *Nat. Genet.*, **2005**,37,138-144.
- 61 K. Sakao, K. A. Takahashi, Y. Arai, M. Saito, K. Honjyo, N. Hiraoka, T. Kishida, O. Mazda, J. Imanishi and T. Kubo. *J. Orthop. Sci.*, **2009**,14,738-747.
- 62 C. D. Richards, C. Langdon, P. Deschamps, D. Pennica and S. G. Shaughnessy. *Cytokine.*, **2000**,12,613-621.

Table 1 Differentially expressed proteins identified by iTRAQ-based quantitative proteomics (↑: up-regulated, ↓: down-regulated).

No.	Accession ID	Symbol	Protein description	CD28 /NC	CD42 /NC	Location
1	D3ZR06	KRT10	Keratin, type I cytoskeletal 10	↓0.48	↓0.71	Cytoplasm
2	G3V7V6	RETSAT	retinol saturase	↓0.54	↓0.62	Cytoplasm
3	G5AX66	GW7_15073	Keratin, type I cytoskeletal 10	↓0.55	↓0.70	Cytoplasm
4	G5ALS8	GW7_03785	Keratin, type II cytoskeletal 1	↓0.58	↓0.73	Cytoplasm
<b>5</b>	<b>Q6AXS5-2</b>	<b>SERBP1</b>	<b>Isoform 2 of Plasminogen activator inhibitor 1 RNA-binding protein</b>	<b>↓0.63</b>	<b>↓0.49</b>	Cytoplasm
6	P07340	ATP1B1	ATPase, Na <sup>+</sup> /K <sup>+</sup> transporting, beta 1 polypeptide	↓0.64	↓0.65	Plasma Membrane
7	D3ZRA3	ACACA	Acetyl-CoA carboxylase 1	↓0.64	↓0.66	Cytoplasm
8	P62744	AP2S1	AP-2 complex subunit sigma	↓0.67	↓0.65	Cytoplasm
9	G3V9G4	ACLY	ATP citrate lyase, isoform	↓0.68	↓0.66	Cytoplasm
10	G5AKR6	NCLN	Nicalin	↓0.68	↓0.74	Plasma Membrane
<b>11</b>	F1LQ93	COL9A1	Collagen alpha-1(IX) chain	↓0.68	↓0.49	Extracellular Space
12	Q0QEW8	RPL18	60S ribosomal protein L18	↓0.69	↓0.67	Cytoplasm
13	P47853	BGN	Biglycan	↓0.69	↓0.73	Extracellular Space
14	G5C9Y3	AKT2	RAC-beta serine/threonine-protein kinase	↓0.69	↓0.66	Plasma Membrane
15	P29266	HIBADH	3-hydroxyisobutyrate dehydrogenase	↓0.70	↓0.75	Cytoplasm
16	O70513	LGALS3BP	Galectin-3-binding protein	↓0.72	↓0.75	Plasma Membrane
17	J7JVB9	MX2	Mx2	↓0.72	↓0.72	Cytoplasm
18	P16975	SPARC	secreted protein, acidic, cysteine-rich	↓0.73	↓0.58	Extracellular Space
19	G5B9E8	TUBA1C	Tubulin alpha-1C chain	↓0.73	↓0.76	Cytoplasm
20	Q6AYD5	GSPT1	G1 to S phase transition 1	↓0.74	↓0.70	Cytoplasm
21	P29314	RPS9	40S ribosomal protein S9	↓0.75	↓0.73	Cytoplasm
22	F1LPS6	IFIT1B	interferon-induced protein with tetratricopeptide repeats 1B	↓0.75	↓0.67	Cytoplasm
23	D3Z9M5	FKBP7	Protein Fkbp7	↓0.77	↓0.76	Cytoplasm
24	Q6AYQ9	PPIC	Peptidyl-prolyl cis-trans isomerase	↓0.77	↓0.70	Cytoplasm
25	D3ZFC6	ITIH4	inter-alpha-trypsin inhibitor heavy chain family, member 4	1.30	1.48	Extracellular Space
<b>26</b>	<b>P03957</b>	<b>MMP-3</b>	<b>matrix metalloproteinase 3</b>	<b>1.31</b>	<b>1.79</b>	<b>Extracellular Space</b>
27	B1WBU9	PYGM	Phosphorylase, glycogen, muscle	1.32	1.37	Cytoplasm
28	F1LTN3		Uncharacterized protein	1.32	1.29	Unknown
29	Q4KM66	LOC500183	similar to NGF-binding Ig light chain	1.33	1.44	Unknown

30	Q64194	LIPA	Lysosomal acid lipase/cholesteryl ester hydrolase	1.33	1.45	Cytoplasm
31	P50339	CMA1	Chymase	1.33	1.38	Extracellular Space
32	F1LTD1		Uncharacterized protein	1.34	1323	Unknown
33	P20761	IGH-1A	Ig gamma-2B chain C region	1.34	1.31	Unknown
34	P20059	HPX	Hemopexin	1.35	1.31	Extracellular Space
<b>35</b>	<b>P02650</b>	<b>APOE</b>	<b>Apolipoprotein E</b>	<b>1.35</b>	<b>1.80</b>	<b>Extracellular Space</b>
36	G5BHR4	FN	Fibronectin	1.36	1.75	Extracellular Space
37	F1LYU4		Uncharacterized protein	1.37	1.36	
38	P14141	CA3	Carbonic anhydrase 3	1.37	1.30	Cytoplasm
39	P51886	LUM	Lumican	1.37	1.70	Extracellular Space
40	P31211	SERPINA6	Corticosteroid-binding globulin	1.38	1.81	Extracellular Space
41	D3ZXR4		Uncharacterized protein	1.38	1.67	
42	D3ZN64	RGD1564680	similar to matrilin 2 precursor	1.39	1.69	unknown
<b>43</b>	<b>Q5XIH1</b>	<b>ASPN</b>	<b>Asporin</b>	<b>1.39</b>	<b>1.92</b>	<b>Extracellular Space</b>
44	P02793	FTL	Ferritin light chain 1	1.40	1.79	Cytoplasm
45	P02600	MYL1	Myosin light chain 1/3, skeletal muscle isoform	1.40	1.32	Cytoplasm
46	Q8K551	ACTN3	Truncated alpha-actinin	1.40	1.49	Plasma Membrane
47	D3ZVB7	OGN	Osteoglycin	1.41	1.69	Cytoplasm
48	F1M8E9	LYZ1/LYZ2	Putative lysozyme C-2	1.42	1.51	Cytoplasm
49	Q63041	PZP	pregnancy zone protein	1.43	1.51	Extracellular Space
50	P08932	KNG1	T-kininogen 1	1.44	1.47	Extracellular Space
51	P04466	MYLPF	Myosin regulatory light chain 2	1.44	1.34	Cytoplasm
52	D3ZWD9		Uncharacterized protein	1.45	1.46	
53	F1LST1	FN1	Fibronectin	1.46	1.86	Extracellular Space
<b>54</b>	<b>G3V7K2</b>	<b>LIFR</b>	<b>Leukemia inhibitory factor receptor</b>	<b>1.46</b>	<b>2.35</b>	<b>Plasma Membrane</b>
55	D3ZKZ1	C8A	Protein C8a	1.48	1.35	Extracellular Space
56	F1M2W3		Uncharacterized protein	1.48	1.45	
57	P09650	MCPT1	Mast cell protease 1	1.48	1.33	Extracellular Space
58	Q66HI5	FTH1	Ferritin, heavy polypeptide 1	1.50	1.7	Cytoplasm
59	F1LMU0	MYH4	Protein Myh4	1.51	1.38	Cytoplasm

60	F1LW65		Uncharacterized protein	1.52	1.33	
61	F1M5H9		Uncharacterized protein	1.56	1.34	
62	Q03626-2	Mug1/Mug2	Isoform 2 of Murinoglobulin-1	1.57	1.61	Extracellular Space
63	F1LQ00	COL5A2	collagen, type V, alpha 2	1.60	1.58	Extracellular Space
64	Q9EQP5	PRELP	proline/arginine-rich end leucine-rich repeat protein	1.61	1.77	Extracellular Space
65	F1LWD0		Uncharacterized protein	1.66	1.31	
66	F2Z3S8	TNNC2	troponin C type 2 (fast)	1.67	1.61	Cytoplasm
67	Q63910	LOC287167	Alpha globin	1.69	1.42	unknown
68	Q5M7V3	IGG-2A	gamma-2a immunoglobulin heavy chain	1.83	2.01	unknown
69	Q9EPH1	A1BG	Alpha-1B-glycoprotein	2.48	4.13	Extracellular Space

Table 2 Individual functions and identified molecules are shown for the “Connective Tissue Disorders” category.

Bio-functions	Diseases annotation	p-value	Activation z-score	Molecules	#molecules
Connective Tissue Disorders	Rheumatic Disease	4.61E-07	1.187	APOE,ASPN,BGN,COL9A1,FN1,LUM,MMP3	7
Connective Tissue Disorders	osteoarthritis	3.56E-05	0.371	ASPN,BGN,COL9A1,LUM,MMP3	5
Connective Tissue Disorders	arthritis	1.84E-05	1.334	A1BG,ACLY,APOE,ASPN,BGN,COL9A1,FN1,FTH1,FTL,LUM,MM P3,SPARC	12
Connective Tissue Disorders	chondrodysplasia	4.24E-03		COL9A1	1
Connective Tissue Disorders	rheumatic disease of joint	5.97E-03		COL9A1	1

Table 3 Network enrichment of molecules within a global Ingenuity Pathway Knowledge Base network.

Molecules in Network	Score	Functions
<b>A1BG</b> , <b>ACACA</b> , Alpha catenin, <b>APOE</b> , <b>BGN</b> , <b>CMA1</b> , <b>COL5A2</b> , <b>COL9A1</b> , <b>collagen</b> , Collagen, type I, <b>Collagen type ix</b> , <b>Collagen type V</b> , Collagen(s), elastase, ERK1/2, <b>Ferritin</b> , <b>FTH1</b> , <b>FTL</b> , <b>HDL</b> , <b>HPX</b> , IL1, <b>ITIH4</b> , Laminin, <b>LDL</b> , <b>LGALS3BP</b> , <b>LIPA</b> , <b>LUM</b> , <b>Lyz1/Lyz2</b> , <b>Mcpt4</b> , <b>MMP3</b> , Pro-inflammatory Cytokine, SAA, <b>SERPINA6</b> , <b>SPARC</b> , Tgf beta	46	Cell-To-Cell Signaling and Interaction, Connective Tissue Disorders, Inflammatory Disease
<b>AP2S1</b> , <b>ASPN</b> , CCDC15, CD99, CEP152, <b>FKBP7</b> , <b>FTL</b> , <b>GSPT1</b> , <b>HIBADH</b> , <b>IFIT1B</b> , IGFBP6, IL12 (family), INTS4, ITFG1, ITGAE, KRT81, <b>LIFR</b> , <b>LOC500183</b> , MYL3, NAGLU, NFKBIA, POLE2, <b>PPIC</b> , PPIH, PRDX4, <b>PYGM</b> , <b>Pzp</b> , RAB25, <b>SERBP1</b> , SRM, STON2, TGFB1, TSSC1, UBC, UBQLN4	29	Developmental Disorder, Hematological Disease, Hereditary Disorder
<b>ACLY</b> , Akt, Alp, Ap1, <b>CA3</b> , CD3, Collagen type IV, Cyclin A, ERK, <b>FN1</b> , IgG, IL12 (complex), Immunoglobulin, Insulin, Jnk, <b>Kng1/Kng1H</b> , Mapk, Mek, <b>Mmp</b> , <b>Mug1/Mug2</b> , <b>MYL1</b> , <b>MYLPF</b> , NFkB (complex), P38 MAPK, Pdgf (complex), PDGF, BB, Pka, Pkc(s), PP2A, <b>RETSAT</b> , <b>RPL18</b> , <b>RPS9</b> , TCR, <b>TNNC2</b> , Vegf	20	Nucleic Acid Metabolism, Small Molecule Biochemistry, Organ Morphology
ACKR3, <b>Actn3</b> , ALDOA, ANXA6, APH1A, ATP1A1, ATP1A3, <b>ATP1B1</b> , ATP5C1, BZW2, DYNC1H1, EGFR, EHMT1, EPCAM, EZH2, FBLN2, FDFT1, ganglioside GM1, GOT, HBA1/HBA2, Hbb-b2, HTT, MACF1, MYH1, <b>MYH4</b> , <b>MYL1</b> , MYL12B, MYL4, MYL6, NDRG2, NEFM, <b>PRELP</b> , PSME1, RPL10A, SERPINA3	9	Organ Morphology, Skeletal and Muscular System Development and Function, Behavior

\*Networks were generated using Ingenuity Pathways Analysis. Each Molecule's identifier was mapped to its corresponding molecule object within the Ingenuity Pathway Knowledge Base (IPKB). These molecules were overlaid onto a global molecular network. Network enrichment of molecules was assessed using a network score (negative log of p-values of Fisher tests). Focus Molecules (in bold) are those identified in our list of differentially expressed genes. Networks shown here are those with network scores > 3.0.

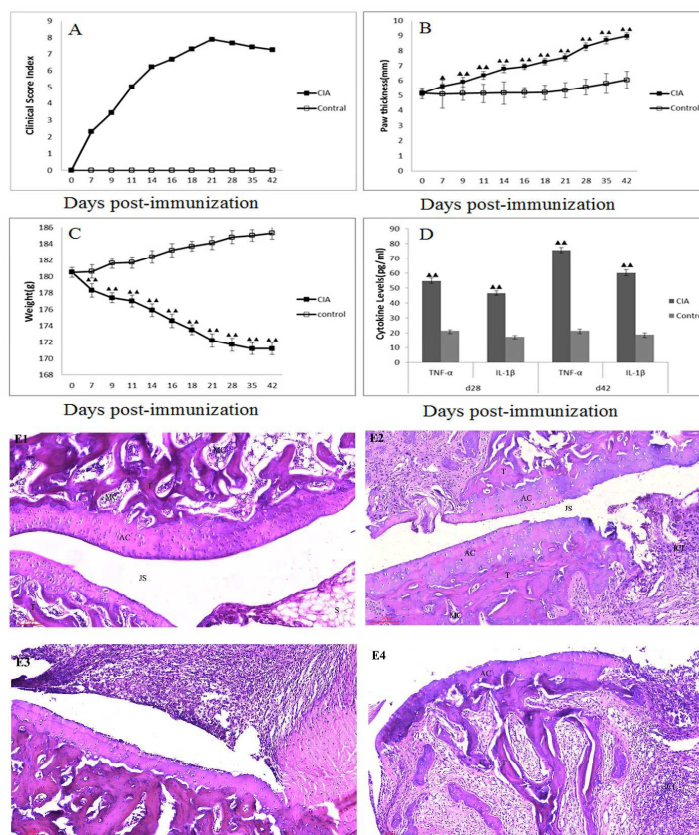


**Fig. 1 Development of arthritis in CIA rats postimmunization and Histological assessment by H&E staining.** Clinical scores (A), paw swelling (B), weight growth (C), and serum inflammatory cytokine levels (D) were compared between normal controls and CIA rats postimmunization. Clinical scores, paw swelling and weight growth parameters were measured 0, 7, 9, 11, 14, 16, 18, 21, 28, 35, and 42 days after immunization ( $n=40$ ), serum inflammatory cytokine were measured 28 and 42 days after immunization ( $n=5$ ). Values represent means  $\pm$  SD,  $\blacktriangle$ = $P < 0.05$ ,  $\blacktriangle\blacktriangle$ = $P < 0.01$  versus the control group. Normal controls (E1), CIA d14 (E2), CIA d28(E3), and CIA d42 (E4) hind ankle joints were evaluated on days 0, 14, 28, and 42 after immunization ( $n = 3-8$ ). The controls had a smooth articular surface with no signs of inflammation. Both CIA d28 and 42 showed thickening of the synovium, inflammatory cell infiltration, and articular cartilage and bone trabeculae destruction, particularly at day 42. CIA d14 displayed less synovial inflammation, indicating a relatively normal joint architecture, scale bar= 100  $\mu$ m. Abbreviations: JC, joint cavity; AC, articular cartilage; T, bone trabeculae; MC, bone marrow cavity; S, synovium; ICI, inflammatory cell infiltrate; E, exudate.

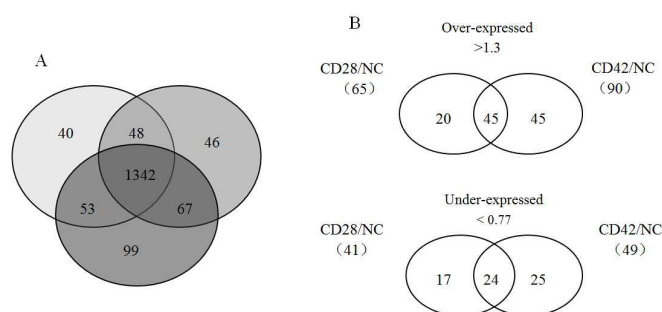


**Fig. 2 CD28, CD42, and NC differentially expressed proteins were analyzed.** (A) A summary of quantitative proteomics in the triplicate experiments is shown. (B) The venn diagram shows the number of overlapping altered proteins between CD28/NC and CD42/NC. The numbers in parenthesis refer to the over- and under-expressed differentially expressed proteins in CD28 and CD42 compared to normal control.

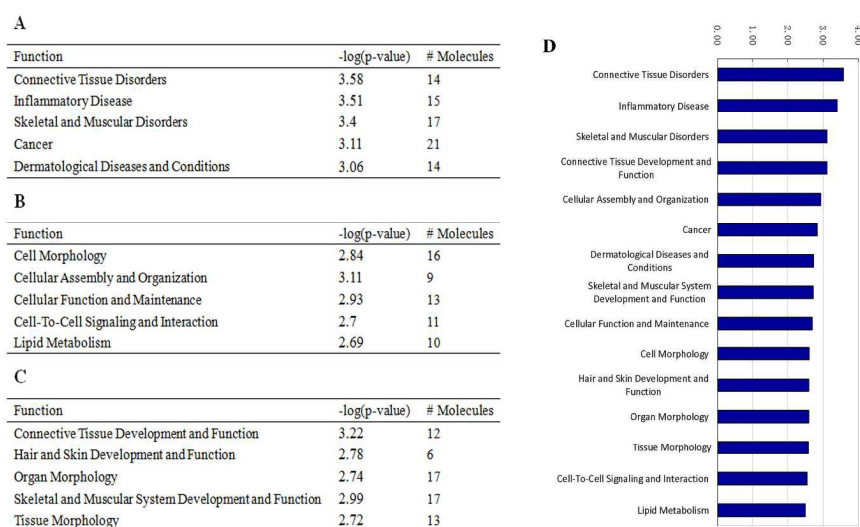


**Fig. 3 The top bio-functions associated with synovial tissue proteomic analysis were identified using IPA.** The bio-functions are listed with the number of molecules and corresponding p-values ( $-\log$ ). (A) Top functions were assigned in the Diseases and Disorders category. (B) Top functions were assigned in the Molecular and Cellular Functions category. (C) Top functions were assigned in the Physiological System Development and Function category. (D) A histogram according to p-values ( $-\log$ ) is shown for the categories. Connective tissue disorders, inflammatory disease, and skeletal and muscular disorders were the top-ranked functions in the three primary categories for proteins discovered in our dataset.

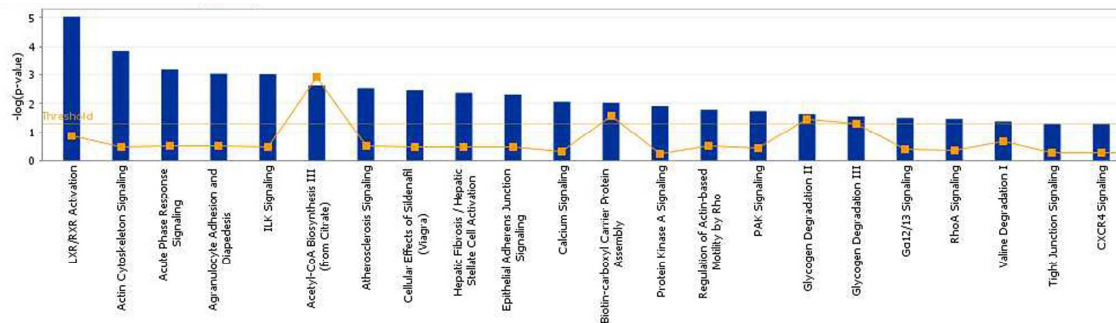


**Fig. 4 Top canonical pathways identified using Ingenuity Pathway Analysis.** A total of twenty two significantly perturbed canonical pathways ( $p < 0.05$ , indicated by threshold line). Yellow line denotes  $-\log(p\text{-value})$  threshold of 1.3 which corresponds to  $p$ -value of 0.05.

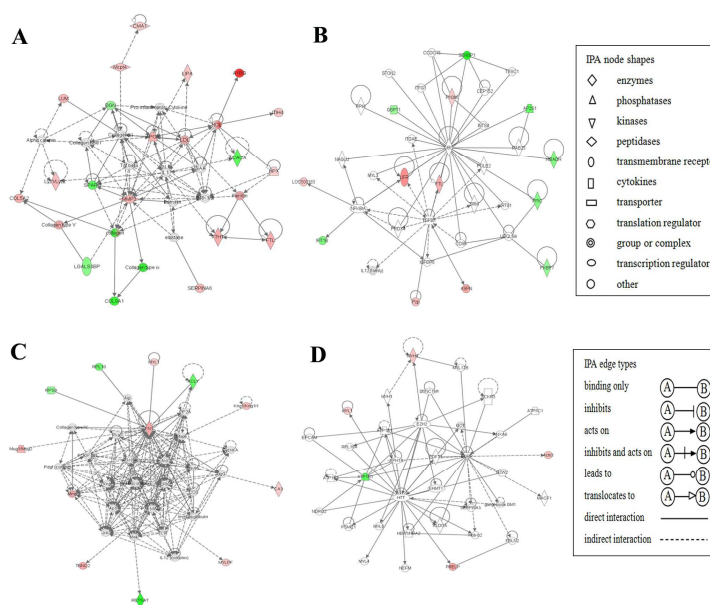


**Fig. 5. Pathway networks were identified using Ingenuity Pathway Analysis.** Network #1 (A), network #2 (B), network #3 (C) and network #4 (D) are shown. The node (protein) and edge (protein relationship) symbols are described in the right of the figures. Colored nodes refer to proteins found in our dataset (pink= upregulated, green=down regulated). Uncolored nodes were not identified as differentially expressed in our experiment and were integrated into the computationally generated IPA networks to indicate relevance to this network.

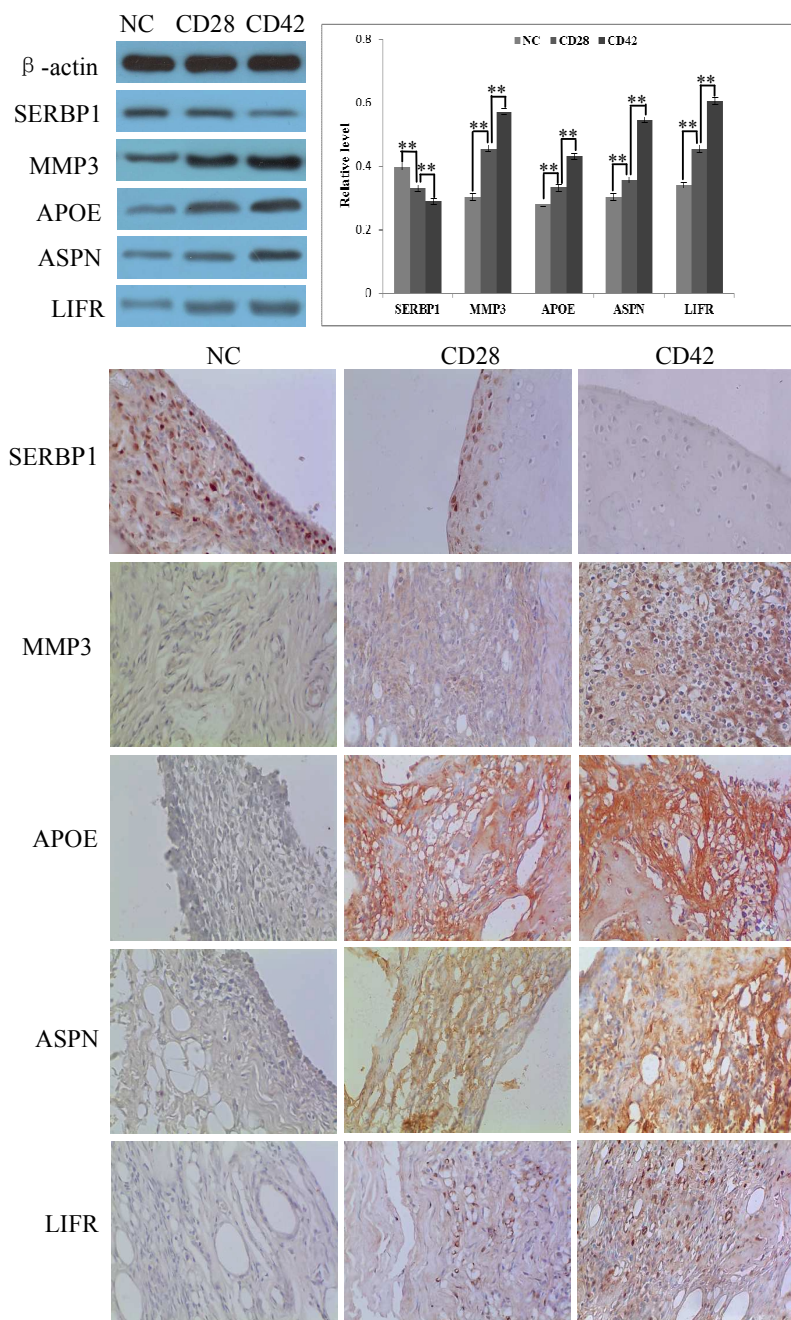


**Fig. 6 Expressional changes of SERBP1, MMP3, APOE ASPN and LIFR within the synovial tissue of CIA and the normal control.** A, (left) a representative result of Western blotting shows the expressions of SERBP1, MMP3, APOE ASPN and LIFR in the synovial tissue of NC, CD28, and CD42; (right) histogram shows the expression levels of the three proteins in the tissues as determined by densitometric analysis.  $\beta$ -actin was used as a loading control. Columns, mean from 10 cases of tissues. Values represent means  $\pm$  SD, \*,  $p < 0.05$ , \*\*,  $< 0.01$ . B, a representative result of immunohistochemistry shows the expression of SERBP1, MMP3, APOE ASPN and LIFR in the synovial tissue of NC, CD28, and CD42. NC= pooled protein samples from the normal control synovial tissue samples. CD28= pooled protein samples from the CIA day 28 synovial tissue samples.

CD42= pooled protein samples from the CIA day 42 synovial tissue samples. Original magnification= 400 $\times$ .